



## Spectroscopy of low lying states in $^{150}\text{Sm}$

A. Saha<sup>a,b</sup>, T. Bhattacharjee<sup>a,b,\*</sup>, S.S. Alam<sup>a,b</sup>, D. Banerjee<sup>c</sup>,  
M. Saha Sarkar<sup>d</sup>, S. Sarkar<sup>e</sup>, J.B. Gupta<sup>f,1</sup>, P. Das<sup>a,b</sup>,  
Soumik Bhattacharya<sup>a,b</sup>, Deepak Pandit<sup>a</sup>, R. Guin<sup>c</sup>, S.K. Das<sup>b,c,1</sup>,  
S.R. Banerjee<sup>a,b</sup>

<sup>a</sup> Variable Energy Cyclotron Centre, Kolkata, PIN-700 064, India

<sup>b</sup> Homi Bhabha National Institute, Mumbai, PIN-400 094, India

<sup>c</sup> RCD-BARC, Variable Energy Cyclotron Centre, Kolkata, PIN-700 064, India

<sup>d</sup> Saha Institute of Nuclear Physics, Kolkata, PIN-700 064, India

<sup>e</sup> Indian Institute of Engineering Science and Technology, Shibpur, West Bengal, PIN-711 103, India

<sup>f</sup> Ramjas College, University of Delhi, Delhi, PIN-110 007, India

Received 29 January 2018; received in revised form 13 April 2018; accepted 7 May 2018

Available online 9 May 2018

### Abstract

Low lying states of  $^{150}\text{Sm}$  have been studied through decay spectroscopy of odd–odd  $^{150}\text{Pm}$ , populated with  $^{150}\text{Nd}(p, n)^{150}\text{Pm}$  reaction at  $E_{\text{beam}} = 8.0$  MeV using 97% enriched  $^{150}\text{Nd}$  target and detecting the  $\gamma$ -rays with the VENUS array comprised of six Compton suppressed Clover HPGe detectors. Nineteen new transitions are placed, four tentative  $\gamma$ -rays are confirmed and eight transitions are found to have altered placements; consequently assigning thirteen new levels to the decay scheme of  $^{150}\text{Pm}$ . The spin-parity assignments of the excited levels of  $^{150}\text{Sm}$  were made based on  $\log ft$  and angular correlation analysis.

© 2018 Elsevier B.V. All rights reserved.

**Keywords:** Decay  $\gamma$  spectroscopy; Decay Half life &  $\gamma - \gamma$  coincidence;  $\log ft$  &  $\gamma - \gamma$  angular correlation; Clover HPGe detectors

\* Corresponding author at: Variable Energy Cyclotron Centre, Kolkata, PIN-700 064, India.  
E-mail address: [btumpa@vecc.gov.in](mailto:btumpa@vecc.gov.in) (T. Bhattacharjee).

<sup>1</sup> Retired.

## 1. Introduction

The study of the low lying states populated through decay spectroscopy may reveal important information on the structure of a nucleus [1–5]. Firstly, the excitation energies and the spins of these states are limited by  $\beta$  decay  $Q$ -value ( $Q_\beta$ ) and the selection rules. As a result, many unique levels can be excited from decay which are otherwise not possible from the nuclear reactions that are suitable to populate the band structures. Secondly, detailed information on these low lying levels and precise measurement of  $\beta$  decay intensity provides a wealth of information regarding the underlying nuclear structure. However, it is very difficult to study such complex decay schemes that are involved with high value of  $Q_\beta$ . The  $^{150}\text{Sm}$  is one such nucleus that can be populated through the  $\beta^-$  decay of  $^{150}\text{Pm}$  ( $Q_\beta = 3454$  keV). The  $\beta$  decay spectroscopy of  $^{150}\text{Pm}$  for studying  $\gamma - \gamma$  coincidence was carried out long back in the year 1970 [6], by using a single crystal Ge(Li) detector for the singles measurement and a well type hollow coaxial Ge(Li) detector for coincidence measurement. Hence, it might be worth revisiting the decay spectroscopy of  $^{150}\text{Pm}$  with high efficiency arrays in order to investigate the excited levels in  $^{150}\text{Sm}$  that are favorably populated from decay.

The  $N = 88$  Sm lies at the transition path of the vibrational to the axially symmetric deformed rotor region and could be associated with the competition between the long-range quadrupole polarizing effects of the nucleon-nucleon force and its short-range part favoring the spherical shapes [7]. Its complex nature is apparent from the varied structures interpreted in this nucleus [8] which also provides a challenge for nuclear theory. Hence, over the time, several experimental and theoretical works have been carried out to enrich the understanding of this nucleus. The experiments include the measurement of singles and coincidence decay spectroscopy [6,9]; angular correlation and directional distribution measurements [10–12]; determination of absolute  $B(E2)$  values [13] and quadrupole moments [14,15] of  $2^+$  states using Coulomb excitation and the measurement of lifetime and electromagnetic transition rates using  $(n, \gamma)$  reaction [16–18]. The results from the lifetime measurements suggested the existence of octupole correlation in this nucleus. The transitions from  $0_2^+$  band to the octupole band was observed [19] and that suggested the co-existence of reflection symmetric and asymmetric octupole shapes in  $^{150}\text{Sm}$ . In theory, Kumar [20] reproduced the shape transition at  $N = 88$ –90 in Sm, Scholten et al. [21] reproduced the variation in the nuclear structure of Sm isotopes with  $N = 86$ –92 and Gupta and Kumar [22] resolved the overlapping character of the  $2_2^+$  and  $2_3^+$  states in the complex spectral features of  $^{150}\text{Sm}$ . Although, the lowest few levels of  $^{150}\text{Sm}$  correspond roughly to those of the vibrational model (VM), the large number of currently known positive parity levels can be grouped into the ground,  $\beta$ ,  $\gamma$ , and  $\beta\beta$  rotational bands [23,24]. The  $0_2^+$  and  $4_1^+$  levels lie at about twice the  $2_1^+$  state energy, but the  $2_2^+$  state lies at more than  $3E(2_1^+)$ . The  $B(E2, 0 \rightarrow 2)$  value drops from  $3.4 e^2b^2$  in  $^{152}\text{Sm}$  to only  $1.2 e^2b^2$  in  $^{150}\text{Sm}$ , but the latter still has a large quadrupole moment  $Q(2_1^+) \sim -1.25$  e-barn. More recently, Gupta et al. [25] also explained the structure of  $^{150}\text{Sm}$  and resolved the anomaly of the shape co-existence. They reproduced the absolute  $B(E2)$  values and the inter-band  $B(E2)$  ratios fairly well by a careful balance of the quadrupole forces and pairing interaction, and predicted the slightly deformed status of  $^{150}\text{Sm}$ , reproducing the quadrupole moment  $Q(2_1^+)$  [14].

In the present work, decay spectroscopy of  $^{150}\text{Pm}$  has been carried out to study the low lying levels in  $^{150}\text{Sm}$ . The decay half lives followed by the observed transitions along with their  $\gamma - \gamma$  coincidence information have been used for the development of level scheme. New levels have been assigned to the decay scheme of  $^{150}\text{Pm}$  with the placement of new transitions, confirming uncertain transitions and also by changing the earlier placements of few transitions. The *logft*

analysis and angular correlation measurement has been utilized to assign/confirm the spin-parity to the excited levels of  $^{150}\text{Sm}$ .

## 2. Experimental Setup and Data Analyzing Techniques

The excited states of  $^{150}\text{Pm}$  were populated by the  $^{150}\text{Nd}(p, n)^{150}\text{Pm}$  reaction using 8.0 MeV proton beams provided by  $K = 130$  AVF cyclotron at Variable Energy Cyclotron Centre (VECC), Kolkata, India. The beam energy was chosen from the measured excitation function for the  $p + ^{150}\text{Nd}$  reaction [26] so as to have maximum cross section for the  $(p, n)$  channel. The  $^{150}\text{Nd}$  target was prepared by electro-deposition technique, starting from commercially available 97.65% enriched powdered oxide sample ( $\text{Nd}_2\text{O}_3$ ), on a 0.3 mil thick aluminium (Al) foil. The isotopic impurities in the target material consisted of 0.50%  $^{142}\text{Nd}$ , 0.31%  $^{143}\text{Nd}$ , 0.68%  $^{144}\text{Nd}$ , 0.23%  $^{145}\text{Nd}$ , 0.47%  $^{146}\text{Nd}$  and 0.26%  $^{148}\text{Nd}$ , as per the data sheet provided by the supplier. The thickness of the targets used in the experiment was  $\sim 900 \mu\text{g}/\text{cm}^2$ . Several targets were irradiated following the stacked foil technique [26]. The irradiated targets were subsequently counted with different configurations of Ge detectors as per the requirement of the decay spectroscopy measurements as discussed below.

In order to measure the decay half lives, the  $\gamma$  decay was followed in singles mode over a period of  $\sim 10$ h where each counting was continued for a duration of 10 minutes. Decay half-life measurement was performed with an isolated Clover HPGe (High Purity Ge) detector and it was also ensured that the detector dead time is kept below 5% during counting. The measurement was performed by using the standard techniques where the background subtracted areas of a particular full energy peak were studied as a function of time. The statistics were increased by adding data files generated during time differentiated counting. The data obtained from this measurement was also used for the measurement of absolute intensities for most of the  $\gamma$ -rays as the absolute efficiency of the detector could be measured with the  $^{152}\text{Eu}$  and  $^{133}\text{Ba}$  sources of known disintegration per second (dps).

In the present work, the decay  $\gamma$  transitions have been detected using the VENUS (VECC Array for Nuclear Spectroscopy) setup of six Compton suppressed Clover HPGe detectors [27] which were placed at a distance of 18 cm from the target and at the angles of  $30^\circ$  (D2),  $90^\circ$  (D3),  $180^\circ$  (D4),  $260^\circ$  (D5) &  $310^\circ$  (D6) w.r.t one of the detectors taken as a reference of  $0^\circ$  (D1). In the  $\gamma - \gamma$  coincidence measurement, conventional two fold coincidence logic was used. The  $\gamma - \gamma$  coincidence data obtained from this setup were used to establish the level scheme. For this purpose, the data were sorted to generate RADWARE compatible  $4\text{k} \times 4\text{k}$  matrix using prompt gating of  $\sim 50$  ns from the total  $\gamma - \gamma$  time events. The random events present within the prompt gate were subtracted by placing gates on the left and right background of the prompt  $\gamma - \gamma$  time peak. This significantly reduced the random coincidence events that may be present in the  $\gamma - \gamma$  coincidence data.

This data were also used for the measurement of  $\gamma - \gamma$  angular correlation at eight different angles. Five equivalent angles ( $90^\circ$  (D3),  $100^\circ$  (D5),  $130^\circ$  (D6),  $150^\circ$  (D2),  $180^\circ$  (D4)) were obtained w.r.t the reference detector at  $0^\circ$  (D1) and the rest three equivalent angles ( $120^\circ$  (D2),  $140^\circ$  (D6),  $170^\circ$  (D5)) were obtained by considering the  $90^\circ$  (D3) detector as the reference detector. The angular correlation coefficients were obtained from the  $\gamma - \gamma$  coincidence data by fitting the coincidence count ( $W(\theta)$ ), corresponding to a particular  $\gamma - \gamma$  cascade, at different angles between the two  $\gamma$ -rays with the following equation:

$$W(\theta) = 1 + A_2 P_2(\cos\theta) + A_4 P_4(\cos\theta)$$

where  $P_2$ ,  $P_4$  are Legendre polynomials and  $A_2$ ,  $A_4$  are the angular correlation coefficients. The theoretical solutions to the  $A_2$  and  $A_4$  coefficients have been obtained, by using the  $F_k$  coefficients [28] corresponding to both the  $\gamma$  decays in a particular cascade, for different values of multipole mixing in one of the transitions. The angular correlation coefficients for the well known 1173–1332 keV (Q–Q) cascade of  $^{60}\text{Co}$  was reproduced and the geometrical correction factor required for this purpose was used for the subsequent measurements.

The pulse processing for the  $\gamma - \gamma$  coincidence measurement was performed by using standard NIM electronics and 32 bit VME ADC. For the singles measurement with the isolated Clover detector, standard NIM electronics and CAMAC ADC were used. All the measurements have been carried out after a cooling time of  $\sim 2$  h or more after the irradiation in order to ensure that all the short lived activities produced during irradiation have decayed out. All the data were gathered in zero suppressed LIST mode using LAMPS [29] and the offline analyses were performed using the LAMPS and RADWARE [30] analysis packages.

### 3. Results

The experimental data were analyzed in order to (i) develop the decay scheme of  $^{150}\text{Pm}$  from the analysis of decay half lives and  $\gamma - \gamma$  coincidence data and (ii) assign the spin-parity ( $J^\pi$ ) to the excited levels of  $^{150}\text{Sm}$  from the analysis of  $\log ft$  values and  $\gamma - \gamma$  angular correlation. The following subsections gives details on the new findings obtained from the present work.

#### 3.1. Decay scheme of $^{150}\text{Pm}$ : Decay Half Life and $\gamma - \gamma$ coincidence

The  $\gamma$  transitions obtained in singles data are shown in Fig. 1. The decay curves exhibited by all the  $\gamma$ -rays were studied in order to identify the origin of each transition. The half lives followed by few representative transitions are shown in Fig. 2. The decay half lives followed by the  $\gamma$ -rays were used for confirming their assignment in the decay scheme of  $^{150}\text{Pm}$ . The coincidence relationships among the  $\gamma$ -rays were also taken into consideration for their final placement in the level scheme. All the transitions identified as belonging to the decay scheme of  $^{150}\text{Pm}$  are tabulated in Table 1 along with the energy of the corresponding excited level of  $^{150}\text{Sm}$ , from which these transitions are decaying. The energies of the  $\gamma$ -rays and excited levels, measured in the present work, are in agreement with the values obtained in ENSDF [23] considering the error involved in the measurement.

The  $\gamma - \gamma$  coincidence analyses were performed with the  $\gamma$ -rays listed in Table 1. The coincidence information related to the well known transitions and levels were verified from the data before placing the new and weak  $\gamma$ -rays in the level scheme. Fig. 3 shows few gated projections on those  $\gamma$  transitions, which are well known in the decay scheme of  $^{150}\text{Pm}$ . The transitions are chosen to have a wide range of intensity values to determine the quality of the data obtained in the present coincidence measurement. The 876.1 keV ( $I_\gamma = 6.52$ ) and 565.4 keV ( $I_\gamma = 1.16$ ) gates show the strong and weak decay branches from the 2069.7 keV level. The 1213.8 keV ( $I_\gamma = 0.89$ ) gate shows the decay of the 2259.6 keV level and the 1647.4 keV ( $I_\gamma = 0.23$ ) gate shows the same for the 2812.7 keV level.

From the present analysis of decay half-life and  $\gamma - \gamma$  coincidence, in total, thirteen new levels were placed in the decay scheme of  $^{150}\text{Pm}$ . Out of these new levels, six levels (viz., 1684.5, 1833.2, 2704.2, 2718.3, 2937.4 and 2987.5 keV) are based on multiple  $\gamma$  decays, most of which are observed for the first time and few have altered placements. The spin-parity of these levels could also be confirmed from  $\log ft$  analysis (cf. Sec. 3.2). Rest of the new levels, assigned to

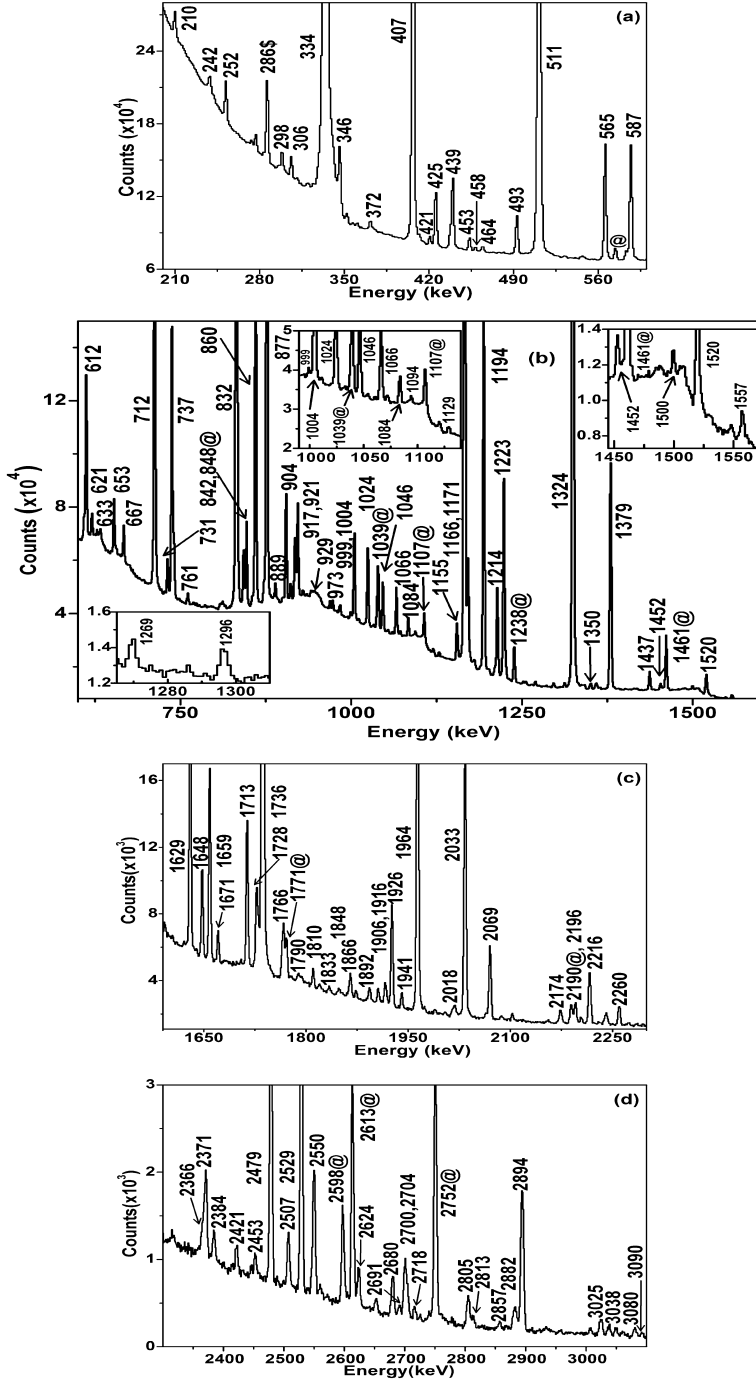


Fig. 1. The singles spectra showing all the transitions observed from the decay measurement. The 286 keV transition, marked with \$, is identified to be arising from the decay of <sup>149</sup>Pm ( $\tau_{1/2} = 53.08(5)$  h). The transitions marked with @ follow longer half lives and have been identified to be coming from background or the contaminations in the Al backing foil.

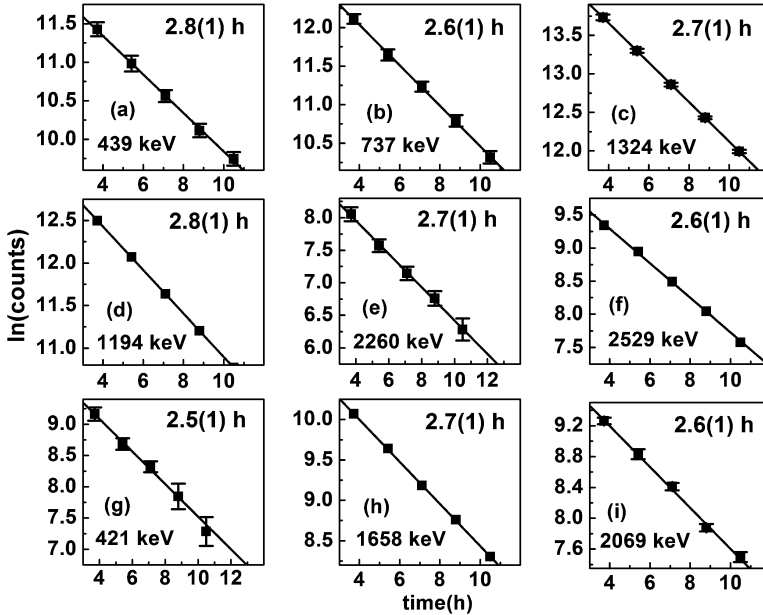


Fig. 2. The decay half lives followed for some of the transitions observed in singles and placed in the level scheme of  $^{150}\text{Sm}$  are shown. (a) 439 keV (773 keV,  $4^+ \rightarrow 334$  keV,  $2^+$ ), (b) 737 keV (1071 keV,  $3^- \rightarrow 334$  keV,  $2^+$ ), (c) 1324 keV (1658 keV,  $2^- \rightarrow 334$  keV,  $2^+$ ), (d) 1194 keV (1194 keV,  $2^+ \rightarrow \text{g.s.}$ ), (e) 2260 keV (2260 keV,  $1^- \rightarrow \text{g.s.}$ ), (f) 2529 keV (2529 keV,  $1^- \rightarrow \text{g.s.}$ ), (g) 421 keV (1194 keV,  $2^+ \rightarrow 773$  keV,  $4^+$ ), (h) 1658 keV (1658 keV,  $2^- \rightarrow \text{g.s.}$ ), (i) 2070 keV (2070 keV,  $2^- \rightarrow \text{g.s.}$ ). Among these (a)–(g) are for the transitions which were already known in  $^{150}\text{Sm}$ ; (h) & (i) for new transitions that are placed in the level scheme of  $^{150}\text{Sm}$ .

the decay scheme of  $^{150}\text{Pm}$ , are based only on a single transition and again four of these levels (viz. 1603.5, 2298.0, 2857.0 and 2882.2 keV) were also known from other reactions but not from  $\beta$  decay [23]. However, no de-exciting  $\gamma$ -ray were known earlier from these four levels. The assigned spin-parity, for the levels which are based only on single transition, are kept in bracket and may be considered as the most probable ones (cf. Sec. 3.2). The following subsections describe the modification made in the level scheme of  $^{150}\text{Sm}$  in the present work, based on the new information obtained with different  $\gamma$ -rays.

### 3.1.1. Modification in the level scheme based on the new transitions

Fig. 4 shows the coincidence relationships of two of the nineteen new  $\gamma$ -rays found in the present work, viz., 1557.4 keV ( $I_\gamma = 0.05$ ) and 1296.3 keV ( $I_\gamma = 0.06$ ) transitions de-exciting the 2298.0 keV and 2367.2 keV levels, respectively. Both these transitions are observed in singles data (see Fig. 1(b)) and follow half-life of  $^{150}\text{Pm}$ . The 1557.4 keV  $\gamma$ -ray, being in coincidence with the 334.1 keV and 406.5 keV transitions (cf. Fig. 4(b)), is placed on top of the 740.6 keV,  $0_2^+$  level, thus, forming the 2298.0 keV level populated from  $\beta$  decay of  $^{150}\text{Pm}$ . One 2294(5) keV,  $3^-$  level is already known in the level scheme of  $^{150}\text{Sm}$  from (p, p'), (d, d') reactions which could possibly be the 2298.0 keV level proposed in the present work. The 1296.3 keV  $\gamma$ -ray was observed in the earlier  $\beta$  decay work but could not be placed in the decay scheme of  $^{150}\text{Pm}$ . In the present work, the 334.1 and 737.2 keV transitions are found to be in coincidence with the 1296.3 keV  $\gamma$ -ray (cf. Fig. 4(a)) and, thus, this transition is placed to be de-exciting from the already known 2367.2 keV level to the 1071.3 keV,  $3_1^-$  level.

Table 1

The excited levels of  $^{150}\text{Sm}$ , populated from  $\beta$  decay of  $^{150}\text{Pm}$  are listed along with the  $\gamma$ -rays de-exciting from these levels. The  $\gamma$ -rays and the excited levels assigned for the first time in the decay scheme of  $^{150}\text{Pm}$  are shown in bold to guide the eye. The  $\gamma$ -rays are marked as: (i) 'a' for new transitions observed in the present work; (ii) 'b' for the transitions with altered placement in the level scheme compared to the earlier  $\beta$  decay work; (iii) 'c' for the tentative transitions known in ENSDF and confirmed in the present work; (iv) 'd' for the transitions confirmed in the present work that could not be placed in the earlier  $\beta$  decay work and (v) 'h' for the transitions with double placement.

$E_x$ (keV)	$J^\pi$		$E_\gamma$ (keV)	$I_\gamma$	$I_{\beta^-}$	$\log ft$	
	Pres. work	Lit. [23]					Pres. work
334.1		$2^+$	334.1	66.40(10.82)	9.4(18)	10.97(2.80)	8.6(1)
740.6		$0^+$	406.5	5.30(88)	1.5(6)	0.33(9)	9.8(1)
773.5		$4^+$	439.4	0.63(12)			
1046.0		$2^+$	305.8	0.10(2)	1.3(4)	0.19(5)	9.9(1)
			711.9	3.63(66)			
			1046.1	0.46(9)			
1071.3		$3^-$	298.2	0.11(2)			
			737.2	1.93(37)			
1165.5		$1^-$	425.3	0.44(7)	25.9(14)	24.12(6.73)	7.7(1)
			831.5	11.03(2.05)			
			1165.5	15.18(2.95)			
1193.6		$2^+$	420.5	0.06(1)	0.6(7)	0.50(14)	9.3(1)
			453.1	0.11(2)			
			859.6	2.97(55)			
			1193.6	4.35(85)			
1255.4		$0^+$	209.5	0.09(1)			
			921.3	0.71(13)			
1417.4		$2^+$	251.9	0.18(3)			
			346.1	0.31(6)			
			<b>371.5<sup>a</sup></b>	0.07(1)			
			1083.5	0.16(3)			
			1417.9	–			
1504.6		$3^+$	310.9	–			
			458.4	0.03(1)			
			731.1	0.20(8)			
			1170.5	0.98(20)			
<b>1603.5</b>	–	( $2^+$ )	<b>1269.4<sup>d</sup></b>	0.04(1)	–	0.04(1)	10.1(1)
1658.2	$2^-(^-)$	$2^-$	241.6	<0.01	19.4(12)	18.74(6.07)	7.4(1)
			464.4	0.05(1)			
			492.5	0.34(6)			
			586.7	1.16(20)			
			611.9	0.78(15)			
			1324.1	16.24(3.23)			
			<b>1658.5<sup>a,h</sup></b>	0.51(10)			
<b>1684.5</b>	$3^-$		910.6	0.15(3)	0.089(25)	0.18(7)	9.4(2)
			1350.4 <sup>c</sup>	0.08(2)			
1713.3	1	$1^-$	548.3	0.04(2)	3.5(3)	3.45(1.08)	8.0(1)
			667.1 <sup>h</sup>	0.20(4)			
			972.5	0.07(1)			
			1379.2	2.89(58)			
			1713.4	0.40(8)			
1786.1	( $\leq 3$ )	$3^-$	620.6	0.11(2)	0.16(4)	0.18(5)	9.3(1)
			1452.4	0.07(2)			
<b>1833.2</b>	( $2^+$ ) <sup>+</sup>		667.1 <sup>b,h</sup>	0.20(4)	–	0.24(5)	9.1(1)
			1499.5 <sup>b</sup>	0.04(1)			
			1833.2	0.02(1)			

(continued on next page)

Table 1 (continued)

E <sub>x</sub> (keV)	J <sup>π</sup>		E <sub>γ</sub> (keV)	I <sub>γ</sub>	I <sub>β<sup>-</sup></sub>		logft
	Pres. work	Lit. [23]			Pres. work	Pres. work	
1963.5	1 <sup>(-)</sup>	1 <sup>-</sup>	<b>892<sup>a</sup></b> 917.2 1222.9 1629.1 1963.6 <sup>h</sup>	<0.01 0.47(9) 2.35(46) 0.84(17) 1.50(31)	5.5(3)	5.11(1.55)	7.6(1)
2069.7	2 <sup>(-)</sup>	2 <sup>-</sup>	<b>237<sup>a</sup></b> 565.4 652.6 876.1 904.2 999.1 <sup>c</sup> 1024.0 1735.7	<0.01 1.16(20) 0.28(5) 6.52(1.22) 0.78(15) 0.05(1) 0.67(13) 5.55(1.34)	17.5(8)	15.25(5.63)	7.0(2)
2259.8	(1 <sup>-</sup> )	1 <sup>-</sup>	<b>2069.4<sup>a</sup></b> 842.1 1004.0 1065.9 1093.8 1213.8 1519.6 1926.1 2259.6	0.26(6) 0.38(9) 0.78(15) 0.41(8) 0.03(1) 0.89(18) 0.29(6) 0.33(7) 0.09(2)	3.26(17)	3.15(89)	7.5(1)
<b>2298.0</b>	3 <sup>-</sup>		<b>1557.4<sup>a</sup></b>	0.05(1)	–	0.05(1)	9.2(1)
2367.2	(3 <sup>+</sup> )	2 <sup>-</sup>	1201.7 <b>1296.3<sup>d</sup></b> 2033.1 <b>2366.4<sup>a</sup></b>	0.03(1) 0.06(1) 1.00(21) 0.03(1)	1.04(9)	1.12(24)	7.8(1)
2507.4	(1 <sup>-</sup> , 2 <sup>+</sup> )	2 <sup>+</sup>	1340.8 2173.7 2507.4	0.03(1) 0.06(1) 0.06(1)	0.58(7)	0.15(4)	8.4(1)
2528.7	1, 2 <sup>+</sup>	1 <sup>-</sup>	1789.6 2195.4 2528.7	0.03(1) 0.09(2) 0.36(8)	0.44(5)	0.48(10)	7.9(1)
2550.4	1 <sup>(-)</sup>	1 <sup>-</sup>	1810.3 2216.3 2550.4	0.05(1) 0.23(5) 0.15(3)	0.39(5)	0.44(9)	7.9(1)
2602.2	(1 <sup>+</sup> , 2, 3)	1 <sup>-</sup>	532.3 <sup>c</sup> 889.0 1436.7 <sup>b</sup>	0.03(1) 0.10(2) 0.23(5)	0.20(3)	0.36(8)	7.9(1)
2679.5	3	(2 <sup>+</sup> )	2679.5 <sup>h</sup>	0.05(1)	0.11(3)	0.05(1)	8.6(1)
<b>2704.2</b>	–	2 <sup>-</sup>	<b>1658.5<sup>a, h</sup></b> <b>1963.6<sup>a, h</sup></b> <b>2370.9<sup>d</sup></b>	0.51(10) 1.50(31) 0.07(2)	–	2.14(44)	6.9(1)
<b>2718.3</b>	3 <sup>-</sup>		<b>2700.4<sup>a</sup></b> <b>2384.2<sup>a</sup></b> <b>2718.0<sup>a</sup></b>	0.06(1) 0.03(1) 0.01(1)	–	0.04(2)	8.6(2)
2812.7	(1 <sup>-</sup> , 2)	2 <sup>-</sup>	1128.8 1154.5 1647.4 1766.4 2478.7 <b>2812.8<sup>a</sup></b>	0.05(2) 0.33(8) 0.23(5) 0.19(4) 0.34(7) 0.01(1)	1.42(10)	1.17(28)	6.9(1)

Table 1 (continued)

$E_x$ (keV)	$J^\pi$		$E_\gamma$ (keV)	$I_\gamma$		$I_{\beta^-}$		$\log ft$
	Pres. work	Lit. [23]		Pres. work	Lit. [23]	Pres. work	Pres. work	
<b>2857.0</b>		(2 <sup>+</sup> , 3 <sup>-</sup> )	2857.0	0.01(1)	–	0.01(1)	8.9(5)	
<b>2882.2</b>	1 <sup>(-)</sup>	(1 <sup>-</sup> )	2882.2	0.03(1)	–	0.03(1)	8.3(2)	
2893.1	(1 <sup>-</sup> , 2)	2 <sup>-</sup>	633.1	0.06(1)	0.61(6)	0.60(14)	7.0(1)	
			<b>929.3<sup>a</sup></b>	0.04(1)				
			1179.9	0.05(1)				
			1727.6	0.22(5)				
			1848.0 <sup>b</sup>	0.02(1)				
			2893.8	0.21(5)				
<b>2937.4</b>	–	1 <sup>-</sup>	<b>1866.1<sup>d</sup></b>	0.08(2)	–	0.12(3)	7.6(1)	
			<b>1892.1<sup>d</sup></b>	0.04(1)				
<b>2958.1</b>	–	(1 <sup>-</sup> )	<b>2624.0<sup>d</sup></b>	0.04(1)	–	0.04(1)	8.0(1)	
<b>2987.5</b>	–	1 <sup>-</sup>	1916.2 <sup>b</sup>	0.07(2)	–	0.12(3)	7.4(1)	
			1940.4 <sup>b,h</sup>	0.05(1)				
3013.6	–	(1 <sup>-</sup> )	2679.5 <sup>h</sup>	0.05(1)	0.19(3)	0.05(1)	7.7(1)	
3024.7	2 <sup>+</sup>		2690.6 <sup>c</sup>	0.01(1)	0.163(24)	0.04(1)	7.8(1)	
			3024.1	0.03(1)				
3037.7	1, 2 <sup>+</sup>	1 <sup>-</sup>	2704.2	0.03(1)	0.10(3)	0.05(2)	7.7(2)	
			3037.7	0.02(1)				
<b>3071.2</b>	–	(1 <sup>-</sup> )	1905.7 <sup>b</sup>	0.04(1)	–	0.04(1)	7.6(1)	
3080.2	1 <sup>(+)</sup>	(2 <sup>+</sup> )	3080.2	0.01(1)	0.102(16)	0.01(1)	8.2(5)	
3090.1	1, 2 <sup>+</sup>	(2 <sup>+</sup> )	3090.1	0.01(1)	0.29(4)	0.01(1)	8.2(5)	
<b>3105.9</b>	–	(1 <sup>-</sup> )	1940.4 <sup>b,h</sup>	0.05(1)	–	0.05(1)	7.4(1)	
3138.8	(1, 2)	(1 <sup>-</sup> )	2804.7	0.04(1)	0.14(3)	0.04(1)	7.4(2)	

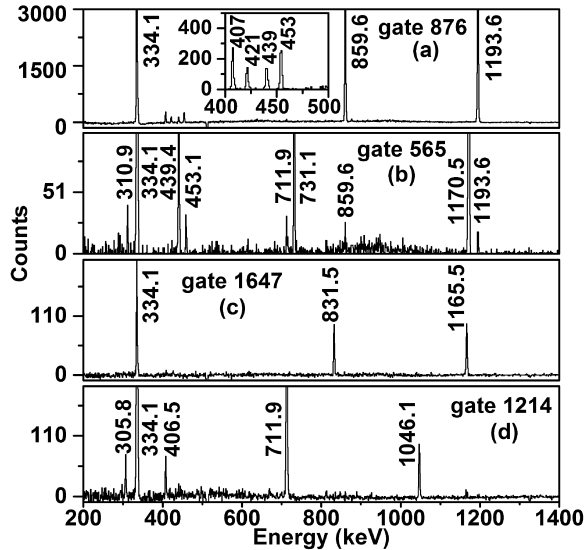


Fig. 3. Gated spectra for some of the transitions which were already known in <sup>150</sup>Sm. (a) 876 keV (from 2069.7 keV, 2<sup>-</sup> level to 1193.6 keV, 2<sup>+</sup> level) gate, (b) 565 keV (from 2069.7 keV, 2<sup>-</sup> level to 1504.6 keV, 3<sup>+</sup> level) gate (c) 1647 keV (from 2812.7 keV, 2<sup>-</sup> level to 1165.5 keV, 1<sup>-</sup> level) gate and (d) 1214 keV (from 2259.6 keV, 1<sup>-</sup> level to 1046 keV, 2<sup>+</sup> level) gate show the known de-excitations in <sup>150</sup>Sm.

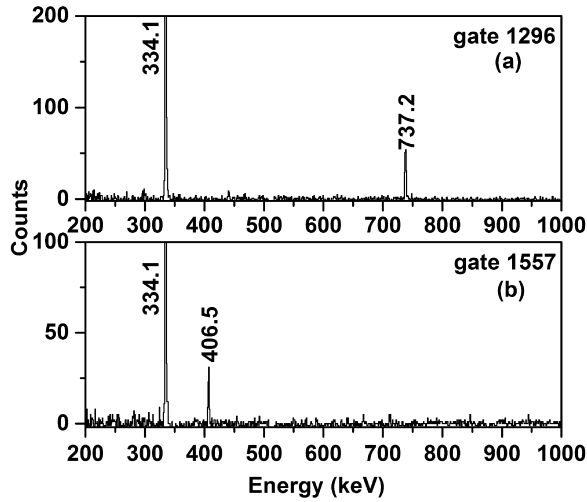


Fig. 4. Gated spectra for some of the new transitions which are placed in the level scheme of  $^{150}\text{Sm}$ . (a) 1296 keV ( $I_\gamma = 0.06$ ; from 2367.2 keV  $2^-$  level to 1071.3 keV,  $3^-$  level) gate and (b) 1557 keV ( $I_\gamma = 0.05$ ; from 2298.0 keV  $3^-$  level to 740.6 keV,  $0_2^+$  level) gate show their placements in the decay scheme of  $^{150}\text{Pm}$ .

Similarly, few more new transitions were observed in the present work which were confirmed from the coincidence data as well as half-life measurement. For example, a 371.5 keV transition is found in the singles data and the 712 keV gated projection shows that it can be placed on top of the 1046.0 keV level. This confirms the connection of the 1417.4 keV,  $2_3^+$  level to the  $2_\beta$  level of  $^{150}\text{Sm}$ . It is important to mention that, although this transition was also observed in some earlier works of Ref. [11,12], it is not mentioned in ENSDF [23].

The 310.9 keV transition, decaying from 1504.6 keV,  $3^+$  level to the 1193.6 keV,  $2_3^+$  level, was not observed in the earlier work on  $\beta$  decay of  $^{150}\text{Pm}$ . This important transition is observed to be in coincidence with the 565.4 keV transition decaying from the 2069.7 keV,  $2^-$  level to this 1504.6 keV level (see Fig. 3(b)).

From  $\gamma - \gamma$  coincidence analysis, the 892 keV  $\gamma$ -ray is found to be in coincidence with 334.1 ( $2_g \rightarrow 0_g$ ) and 737.2 ( $3^- \rightarrow 2_g$ ) keV transitions. Hence, this new  $\gamma$ -ray is placed in the level scheme of  $^{150}\text{Sm}$  and it de-excites the 1963.5 keV level to the 1071.3 keV,  $3^-$  level.

A new 929.3 keV transition is found from the present experiment which is in coincidence with 334.1, 406.5, 1222.9, 1629.1 and 1963.6 keV transitions, as per the 1223 and 1964 keV gated projections. This indicates that the 929.3 keV  $\gamma$ -ray is de-exciting from the 2893.1 keV level to the 1963.5 keV,  $1^-$  level.

Two new  $\gamma$ -rays, viz., 2069.4 keV and 2812.8 keV, have been observed in singles data which follow the half-life of  $^{150}\text{Pm}$  (see Fig. 2) but have no coincidence with the  $\gamma$ -rays of  $^{150}\text{Sm}$ . These transitions are proposed to be feeding directly to the ground state as the 2069.7 keV and 2812.7 keV levels are already known in the level scheme. A 237 keV transition is also observed for the first time in the decay of  $^{150}\text{Pm}$  and this could be placed as de-exciting the 2069.7 keV level and placed on top of the 1833.2 keV,  $(2)^+$  level, as per 667 and 1499 keV gated projections.

The 1269.3(10) keV transition was observed in the earlier  $\beta$  decay work [6] but could not be placed in the level scheme. A 1269.4 keV transition is found in the present work as well

(Fig. 1(b)) following  $^{150}\text{Pm}$  decay half-life. This  $\gamma$ -ray is found to be in coincidence with the 334.3 keV  $\gamma$ , thus, possibly de-exciting the 1603.5 keV level to the 334.1 keV,  $2^+$  level. A 1603(4) keV level was also observed in (p, t) reaction [23,31].

A 2384.2 keV transition, observed for the first time, could be placed on top of the 334.1 keV,  $2_1^+$  level based on decay half-life and coincidence measurements and is, thus, decaying from a 2718.3 keV,  $3^-$  excited level. The population of this level is also indicated by the observation of a 2718 keV transition following half-life similar to that of  $^{150}\text{Pm}$ . One 2715(4) keV,  $3^-$  level is known in  $^{150}\text{Sm}$  from the (p, p') and (d, d') reactions [23]. However, no  $\gamma$  transition was known to be decaying from this level. The newly observed 2718.3 keV level could be same as this 2715(4) keV level of Ref. [23]. However, a 2715.5 keV level is proposed in the recent (p, t) experiment [31] that decays through a 1522 keV transition to the 1193.6 keV,  $2_3^+$  level. In the present work, no 1522 keV transition is observed that satisfies the population of 2715.5 keV level proposed in Ref. [31]. Instead, a 1519.6 keV transition is observed in singles (Fig. 1(b)) which follow the half-life of  $^{150}\text{Pm}$  but shows coincidence with 334.1 and 406.5 keV transitions (Fig. 8). Hence, this  $\gamma$ -ray has been placed on top of the 740.6 keV,  $0_2^+$  level and is, thus, decaying from the 2259.8 keV,  $1^-$  level (cf. Table 1).

Two  $\gamma$  transitions of energy 2857.0 and 2882.2 keV are observed in the singles data out of which the 2882.2 keV  $\gamma$  is found to follow the half-life similar to  $^{150}\text{Pm}$ . The half-life followed by the other transition could not be determined due to low statistics. One 2861(7) keV level is proposed in ENSDF which were observed in (n,  $\gamma$ ) and (d, p) reaction. The 2880.9(5) keV level proposed in ENSDF were observed in ( $\gamma$ ,  $\gamma'$ ) data. The observation of 2857.0 keV and 2882.2 keV transitions in singles data might indicate the population of the above two excited levels from the  $\beta$  decay of  $^{150}\text{Sm}$ .

In the earlier  $\beta$  decay work, transitions of energy 1865.2(10) and 1893.2(10) keV were observed but were not placed in the level scheme. Two transitions of energy 1866.1 and 1892.1 keV, are found also in the present work from both singles and coincidence data. Their coincidence relationships show that they may de-excite from 2937.4 keV level to the 1071.3 keV,  $3^-$  and 1046.0 keV,  $2^+$  levels respectively. It is worth mentioning here that a 2937(20) keV level is already known in the adopted level scheme of  $^{150}\text{Sm}$  which was suggested in three different experiments with (p, t), (d, p) and (n,  $\gamma$ ) reactions.

The 2624 keV transition, observed in the present and earlier  $\beta$  decay work, is found to follow half-life close to the half-life of  $^{150}\text{Pm}$ . This transition is in coincidence with 334.1 keV and, thus, belongs to the level scheme of  $^{150}\text{Sm}$ . This suggests that there could be a 2958.1 keV state in the level scheme of  $^{150}\text{Sm}$  which is proposed for the first time.

### 3.1.2. Modification in the level scheme based on altered and double placements of $\gamma$ -rays

Similar to the case for placements of new  $\gamma$ -rays, Fig. 5 and Fig. 6 show the coincidence for the transitions which are found to have altered and double placements, respectively. The presence of 831.5 and 1165.5 keV transitions in the gated projection of 1436.7 keV ( $I_\gamma = 0.23$ ) suggests the altered placement of this transition. This, along with 1766.4 keV  $\gamma$ -ray, decaying out of the 2507.6 keV,  $2^+$  level as per ENSDF, is found to have different placement according to the present  $\gamma - \gamma$  analysis. The doubles gate of 1436.7 keV transition shows that this  $\gamma$ -ray sits over 1165.5 keV,  $1^-$  level instead of 1071.3 keV,  $1^-$  (see Fig. 5(a)). Hence, the placement of this transition is changed and is found to be de-exciting from the 2602.2 keV,  $1^-$  level. The 1766.4 keV transition is found to have a single placement in the level scheme which is on top of the 1046.0 keV,  $2^-$  level. Also, the 848 keV transition, earlier known to be decaying from this

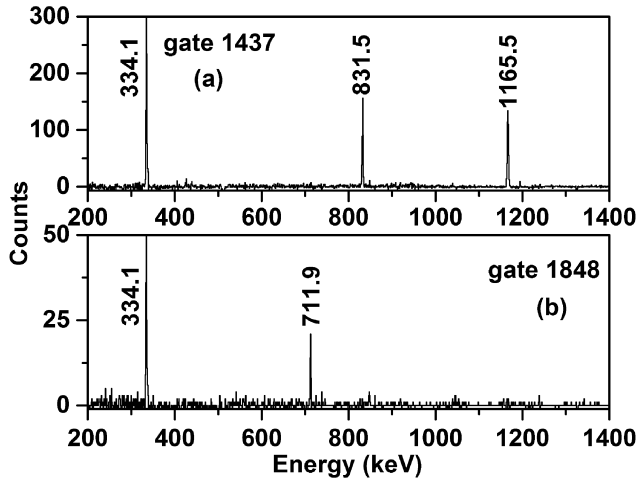


Fig. 5. Gated spectra for some of the transitions for which the placement has been changed in the level scheme of  $^{150}\text{Sm}$ , based on  $\gamma - \gamma$  coincidence and (a) 1437 keV ( $I_\gamma = 0.23$ ; from 2602.2 keV,  $1^-$  to 1165.5 keV,  $1^-$  level) gate, (b) 1848 keV ( $I_\gamma = 0.02$ ; from 2893.1 keV,  $2^-$  level to 1046.0 keV  $2^+$  level) gate.

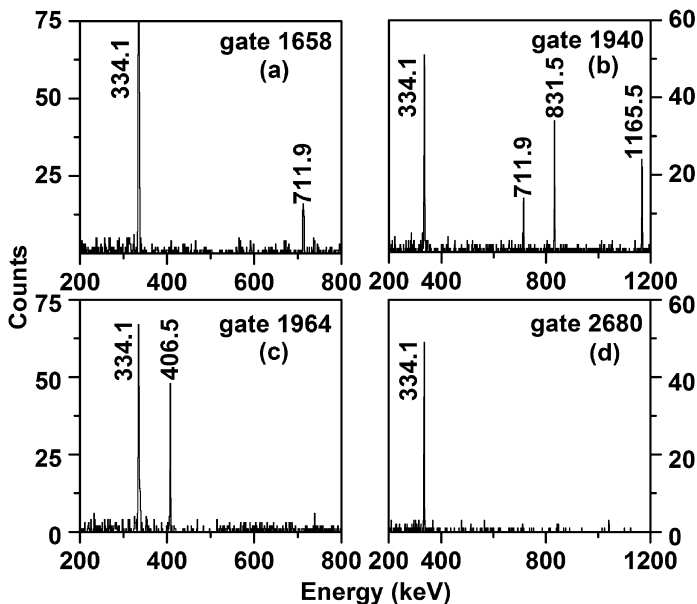


Fig. 6. Gated spectra for some of the transitions which are doubly placed in the level scheme of  $^{150}\text{Sm}$ . (a) 1658 keV transition de-exciting both the 1658.2 keV and 2704.2 keV levels. This is also a new transition observed in the present work. (b) 1940 keV transition de-exciting the 2987.5 keV and 3105.9 keV levels. (c) 1964 keV  $\gamma$ -ray de-exciting both the 1964.8 keV level and 2704.9 keV level. The 1964 keV de-excitation from the 2704.2 keV level is proposed for the first time. (d) The 2680 keV gate shows that this transition also decays from the 3013.6 keV level in addition to the 2679.5 keV level proposed in earlier  $\beta$  decay work [6].

2507.4 keV level, is found to follow a much longer half-life and is confirmed to be originated from contamination in Al backing foil from coincidence data.

Similarly, from the 1848 keV gate, the altered placement of this transition is understood. The 1507.1, 1848.0 and 1940.6 keV transitions were earlier known to be de-exciting a 3012.3 keV level to 1504.6 keV,  $3_1^+$ ; 1165.5 keV,  $1^-$  and 1071.3 keV,  $3^-$  levels respectively, as per the  $\beta$  decay spectroscopy of  $^{150}\text{Pm}$  [6]. Out of these  $\gamma$ -rays, the 1848 and 1941 keV  $\gamma$ -rays are observed to have different placements in the level scheme from the  $\gamma - \gamma$  coincidence data of the present work (see Fig. 5 and Fig. 6). The gated projection of the 1848 keV transition (see Fig. 5(b)) has 334.1 and 711.9 keV  $\gamma$ -rays in coincidence. The non-observation of 1046 keV transition in this gated spectrum could be justified from its intensity ratio compared to the 711.9 keV  $\gamma$ -ray in singles and other gated projections. Hence, the 1848 keV transition is placed on the top of 1046.0 keV,  $2^+$  level and, thus, de-excites the 2893.1 keV level instead of 3012.3 keV. The gated spectrum of 1940.4 keV  $\gamma$ -ray also shows that this transition is in coincidence with 334.1 and 711.9 keV but not with 737.5 keV. Hence, the 1940.4 keV transition is placed on top of the 1046.0 keV,  $2^+$  level, thus, populating the 2987.5 keV level. The 1940.4 keV  $\gamma$ -ray is also found to have double placement in the level scheme and this transition is de-exciting from both the 2987.5 keV,  $1^-$  and 3105.9 keV,  $1^-$  levels to 1046.0 keV,  $2^+$  and 1165.5 keV,  $1^-$  levels, respectively. The latter level of 3105.9 keV,  $1^-$  was not known earlier in the level scheme of  $^{150}\text{Sm}$  and is proposed for the first time. Also, as the presence of 1507.1 keV transition could not be confirmed from the coincidence analysis, the existence of the 3012.3 keV level in the decay scheme of  $^{150}\text{Pm}$  could not be established. However, the 3013.6 keV level was observed in the present work which is de-excited with the emission of a 2679.5 keV  $\gamma$ -ray to the 334.1 keV level. This is confirmed from the coincidence analysis. Also, in the earlier  $\beta$  decay work [6], one dotted 2679.5 keV transition was shown to be de-exciting the 2679.5 keV level which could not also be negated from the present experiment.

With a similar analysis of the 1906 keV gate, it was found that this transition is to be placed on top of the 1165.5 keV,  $1^-$  level and not 1193.6 keV,  $2^+$  level, as it is neither in coincidence with 1193.6 nor 859.6 keV  $\gamma$ ; but in coincidence with the 334.1, 831.5 and 1165.5 keV transitions. This transition was earlier known to be de-exciting the 2679.5 keV level but the present work shows that the transition is decaying from 3071.2 keV,  $1^-$  level to the 1165.5 keV,  $1^-$  level. The 3071.2 keV level is proposed for the first time in the level scheme of  $^{150}\text{Sm}$ .

A 1658.5 keV transition has been observed in singles which follows half-life of  $^{150}\text{Pm}$  ground state (see Fig. 2(h)). Hence, this  $\gamma$ -ray has been placed on the ground state as there is a 1658.2 keV level already known in the level scheme of  $^{150}\text{Sm}$ . However, the gated projection of 1658 keV (Fig. 6(a)) shows that this transition is in coincidence with 334.1 and 711.9 keV  $\gamma$ -rays. This indicates that 1658 keV has a double placement, de-exciting both the 1658.5 and 2704.2 keV levels to the 0.0 keV,  $0_g$  and the 1046.0 keV,  $2_\beta$  levels respectively. The intensity of this transition is found to be  $\sim 0.5\%$  compared to 334.1 keV transition which may be contributed by the summed intensity of two  $\gamma$ -rays present in the decay of  $^{150}\text{Pm}$ .

Similarly, the 1963.6 (Fig. 6(c))  $\gamma$ -ray is in coincidence with 334.1 and 406.5 keV lines and this confirms the de-excitation of 2704.2 keV level also by 1963.6 keV  $\gamma$ -ray to the 740.6 keV,  $0^+$  level. The 2704.2 keV level, which is de-excited by the 2370.9 keV transition, might be same as the 2701.3(5) keV level that was earlier observed in the  $(\gamma, \gamma')$  experiment [23]. A 2700.4 keV transition is observed as doublet with another 2704.2 keV  $\gamma$ -ray. The latter transition is found in 334.1 keV gate and is, thus, assigned to be decaying from the 3037.7 keV,  $1^-$  level. The 2700.4 keV transition, however, is not present in the coincidence data and might indicate the population of a 2701 keV level in  $\beta$  decay of  $^{150}\text{Pm}$ . The energy of this transition shows a dif-

ference of nearly 3 keV compared to the 2704.2 keV level under discussion and this conjectures the existence of more than one discrete energy levels around 2702 keV. However, in the present work, this  $\gamma$ -ray is listed as decaying from the 2704.2 keV level only.

The 1916.2 keV transition, following similar half-life as  $^{150}\text{Pm}$ , is found to be in coincidence with only 334.1 and 737.2 keV  $\gamma$ -rays. This transition has no coincidence with the 1165.5 and 831.5 keV transitions and, thus, can not de-excite the 3080.2 keV level, as placed earlier. Hence, this transition is placed on top of the 1071.3 keV,  $3^-$  level and, thus, de-excites the 2987.5 keV level. This level is proposed for the first time in the present work.

The gated projection of the 667.1 keV transition, known to be de-exciting the 1833.2 keV level to the 1165.5 keV,  $1^-$  level (as per ENSDF), shows that it has a double placement in the level scheme. In addition to its placement above 1046.0 keV level, this transition is in coincidence with the 1165.5 keV and 831.5 keV  $\gamma$ -rays. Hence, this suggests the population of the 1833.2 keV,  $(2)^+$  level from the  $\beta$  decay of  $^{150}\text{Pm}$  as well. The population of this level is also supported by the observation of the 1499.5 keV transition (Fig. 1(b)) which is known as de-exciting from the 1833.2 keV level to the 334.1 keV level, as per the ENSDF data [23]. The 1499.5 keV transition shows coincidence only with the 334.1 keV  $\gamma$ -ray but no other low lying transitions in  $^{150}\text{Sm}$  level scheme. In the earlier  $\beta$  decay work also, a 1499 keV transition was observed but that was placed on top of the 1713.3 keV level. The 1833.2 keV transition is observed in the singles data which also confirms the population of 1833.2 keV level from  $\beta$  decay of  $^{150}\text{Pm}$  which was earlier known from the  $\epsilon$  decay of  $^{150}\text{Eu}$ .

### 3.1.3. Modification based on confirmation of tentative transitions

Fig. 7 shows the gated projections for some of the tentative  $\gamma$  lines which are confirmed in the present work. The placement of the 1350.4 keV transition, which was tentatively placed as de-exciting the 1684.5 keV,  $3^-$  level to the 334.1 keV,  $2^+$  level in the earlier  $\beta$  decay work [6], is confirmed from the coincidence measurement (cf. Fig. 7(c)) and by following its decay half-life. It is also observed that the 1350.4 keV  $\gamma$ -ray has a single placement in the level scheme of  $^{150}\text{Sm}$  as the coincidence data could not confirm the second placement of the 1350.4 keV  $\gamma$ -ray decaying from the 3138.8 keV level to the 1786.1 keV level. The 999.1 keV transition which was tentatively placed as decaying from the 2069.7 keV,  $2^-$  level to the 1071.3 keV,  $3^-$  level is also observed in the present work (Fig. 1(b)). This  $\gamma$ -ray follows half-life comparable to that of  $^{150}\text{Pm}$  and its coincidence gate confirms its placement in the level scheme of  $^{150}\text{Sm}$ . Similarly, the 2690.6 keV transition, which had a tentative placement in the level scheme, is found to be in coincidence with the 334.1 keV  $\gamma$ -ray and, thus, confirming the placement of this transition from the 3024.7 keV level to the 334.1 keV,  $2_g$  level. Similarly, the tentative placement of the 532.3 keV transition could be confirmed to be de-exciting from the 2602.2 keV level using  $\gamma - \gamma$  coincidence data. However, the second placement of this 532.3 keV  $\gamma$ -ray, de-exciting the 3212.5 keV level, could not be confirmed and the present work suggests that 532.3 keV has only a single placement in the level scheme.

### 3.1.4. Level structure around 2260 keV level

All the eight transitions reported to be de-exciting the 2259.8 keV level, by Barrette et al. [6], have been observed in the present work in contrast to the recent observation made by Humby et al. [31] who observed only one out of the eight transitions, viz., 1926.1 keV. From the  $\gamma - \gamma$  coincidence measurement, performed in the present work, the placement of all these eight transitions could be confirmed as de-exciting the 2259.8 keV level. These spectra are shown in

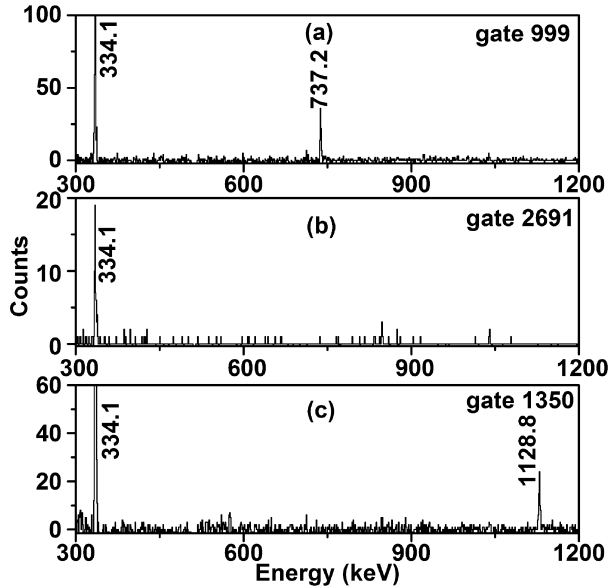


Fig. 7. Gated spectra for some of the transitions which were placed as dotted in earlier works [23] but confirmed in the present work. (a) 999 keV ( $I_\gamma = 0.05$ ; from 2069.7 keV,  $2^-$  to 1071.3 keV,  $3^-$  level) gate, (b) 2691 keV ( $I_\gamma = 0.01$ ; from 3024.7 keV,  $2^+$  to 334.1 keV,  $2^+$  level) gate and (c) 1350 keV ( $I_\gamma = 0.08$ ; from 1684.5 keV,  $3^-$  to 334.1 keV,  $2^+$  level) gate confirm the transitions which were earlier placed as dotted.

Fig. 3(d) and Fig. 8. Hence, the present work does not support the propositions made in Ref. [31] in which the possibility of the existence of multiple discrete states near 2260 keV was suggested.

### 3.2. $J^\pi$ assignments for the excited levels of $^{150}\text{Sm}$

The spin-parity assignment to the observed levels in  $^{150}\text{Sm}$  have been done based on the  $\log ft$  and  $\gamma - \gamma$  angular correlation analysis as described in the following subsections 3.2.1 and 3.2.2. The  $J^\pi$  assignments that are made from the present work are shown in Table 1 in comparison to the spin-parity known from ENSDF data base. In the present work,  $J^\pi$  value is assigned/confirmed for twenty eight levels in  $^{150}\text{Sm}$  for which the spin-parity was either not known or uncertain. The following sections describe the methods of analysis and the salient observations made in the present work.

#### 3.2.1. $\log ft$ analysis

The modification in level scheme obtained in the present work calls for re-determination of  $\beta$  decay branching intensities associated to different known and the new excited levels in  $^{150}\text{Sm}$ . For this purpose, the relative intensities of the  $\gamma$  transitions have been estimated with respect to the 334.1 keV ( $2^+ \rightarrow 0^+$ ) transition after correcting for the 10%  $\beta$  decay branching of  $^{150}\text{Pm}$  to the ground state of  $^{150}\text{Sm}$  [23]. The  $\gamma$ -ray intensities derived in the present work have been used to estimate the  $\beta$  decay branching to different levels and the same has been compared with the earlier work (cf. Table 1). The  $\beta$  branching intensities so obtained have been used to estimate the  $\log ft$  values by using the  $\log ft$  calculator available in NNDC [32].

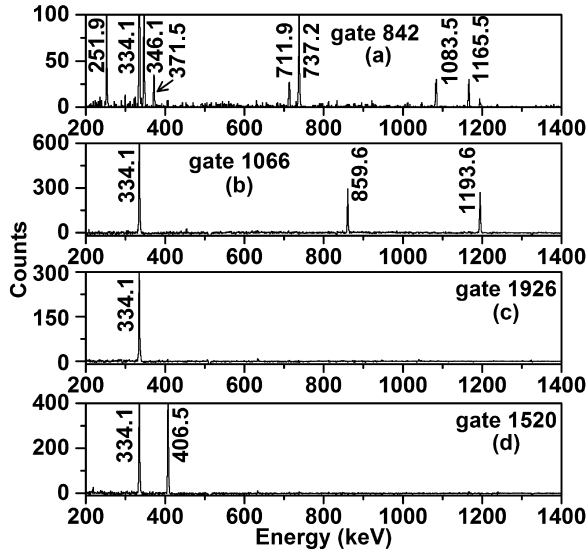


Fig. 8. Gated spectra for some of the transitions de-exciting the 2260.7 keV level for which the placement has been confirmed in the present work.

The ground state of  $^{150}\text{Pm}$  has been evaluated as  $1^-$  in ENSDF [23]; suggested as  $2^-$  in the work of D. Bucurescu et al. [33] and as  $1^-$  or  $2^-$  in the work of Barrette et al. [6]. In the present work, the 1684.5, 2298.0 and 2718.3 keV levels of  $^{150}\text{Sm}$  are observed to be populated from  $\beta$  decay of  $^{150}\text{Pm}$  and the  $J^\pi$  assignments of  $3^-$  to these three levels are confirmed from earlier works [23]. The  $1^-$  assignment to the ground state of  $^{150}\text{Pm}$  does not corroborate with the  $3^-$  spin-parity of these levels of  $^{150}\text{Sm}$ , considering the  $\log ft$  values obtained for these levels (8.6(2), 9.2(1) and 9.6(2) respectively) and the corresponding range (10.6–14.2 for the  $\Delta J = 2$ ,  $\Delta\pi = \text{'no'}$  decays) given for that in  $\beta$  decay  $\log ft$  table [34]. The  $\log ft$  values obtained for all these three levels and their known  $3^-$  assignment supports, however, the  $J^\pi = 2^-$  for the ground state of  $^{150}\text{Pm}$ . Hence, the spin-parity of  $2^-$  is considered for the ground state of  $^{150}\text{Pm}$  while assigning the  $J^\pi$  values to the excited levels of  $^{150}\text{Sm}$  based on the  $\log ft$  values.

The  $\beta$  decay  $\log ft$  table [34] has been used for this assignment and the  $J^\pi$  of the excited levels of  $^{150}\text{Sm}$  are given in Table 1. The  $\log ft$  values for the levels with known spin-parity have also been taken as a guiding factor. For instance, the  $\log ft$  value for the 1165.5 keV level, for which the  $J^\pi$  value is already known as  $1^-$ , comes out to be 7.7(1). Taking this as a guiding factor, the  $J^\pi$  value for the 1963.5 keV level has been assigned as  $1^-$  which was shown as  $1^{(-)}$  in the adopted level scheme. Similar is the case for the other levels with different spin-parity. References have also been taken from the considerations made in earlier experiments. It is worth mentioning that the  $\log ft$  values obtained for most of the levels, with already known  $J^\pi$ , lie on the higher side of the range of values provided in Ref. [34]. Also, for many of the levels, the obtained  $\log ft$  values indicate the presence of Gamow-Teller (GT) type of  $\beta$  decay of  $^{150}\text{Pm} \rightarrow ^{150}\text{Sm}$ .

Fifteen excited levels, observed in the present work, were found to have  $\log ft$  values close to 7.7(1), the  $\log ft$  value that has been obtained for the 1165.5 keV level. These levels were assigned to have  $J^\pi = 1^-$  based on the known  $1^-$  assignment of the 1165.5 keV level. Among these, the  $J^\pi$  assignment to the 2528.7 and 2550.4 keV levels as  $1^-$  from the  $\log ft$  analyses also supports the proposition made by Barrette et al. [6].

For six of the excited levels,  $J^\pi = 2^-$  assignments were made from the present work. Out of these, the  $2^-$  assignment of three levels, viz., 1658.2, 2069.7 and 2367.2 keV, are also supported by the angular correlation analysis. In the present work, the direct decay of all these six  $2^-$  levels to the  $0^+$  ground state are observed. The  $\gamma$  transitions which are connecting these  $2^-$  levels to the  $0^+$  ground state will be either M2 or E3 in nature. The M2 assignments to any of these transitions would, however, imply the level lifetimes  $\sim$  few picoseconds (ps) to hundred ps, as was also discussed for the 2812.7 keV,  $2^-$  level, in the earlier  $\beta$  decay work [6].

The  $J^\pi = 2^+$  assignment has also been made for five of the levels in  $^{150}\text{Sm}$ , by comparing their  $\log ft$  values with that of 1046 keV,  $2^+$  level. For some of these  $2^+$  levels, viz. 2507.4, 2679.5, 3080.2 and 3090.1 keV, their direct decay to the  $0^+$  ground state was also taken into consideration and the corresponding  $\gamma$ -rays were assigned to have E2 multipolarity. The  $J^\pi$  assignment of  $2^+$  for the 2679.5 keV level is based on the estimated  $\log ft$  value by considering the decay of this level through a single 2679.5 keV  $\gamma$ -ray. The  $2^+$  assignment to the 2679.5 keV level was also suggested in the earlier  $\beta$  decay spectroscopy, based on the connection of this level to the 773.5 keV,  $4^+$  level in  $^{150}\text{Sm}$ . However, in the present work, none of the transitions other than the direct ground state decay by 2679.5 keV could be confirmed from the  $\gamma - \gamma$  coincidence measurement. Hence, the  $J^\pi$  value corresponding to this level has been shown in bracket. Similar treatment was adopted for all those levels which are based on the decay of a single  $\gamma$ -ray as the present work could not rule out the possibility of further modification of the decay of these levels.

In the present work, the  $J^\pi = 3^-$  assignment was made to only one excited level, viz., 1786.1 keV level for which the spin was known as  $\leq 3$  and no parity was assigned. The present assignment is made by comparing the  $\log ft$  value obtained for this level to those of the 1684.5 and 2298.0 keV  $3^-$  levels. Also it is considered that the  $3^-$  assignment to the 1786.1 keV levels allows the 620.6 keV and 1452.4 keV  $\gamma$  decays from this level to the 1165.5 keV,  $1^-$  and  $2^+_1$  levels, respectively, and these transitions could be E2 and E1 in nature. The 2857 keV level was also assigned a  $J^\pi = (2^+, 3^-)$  from the derived  $\log ft$  value.

### 3.2.2. $\gamma - \gamma$ angular correlation measurements

In Fig. 9, the experimental values of angular correlation coefficients ( $A_2, A_4$ ) are shown together with some of the theoretical solutions as a function of mixing ratio ( $\delta$ ) in order to determine the appropriate spin value for a particular level in the cascade. The theoretical solutions correspond to the ellipses shown in the figure when one of the correlated  $\gamma$ -ray is considered to have the admixtures of two multipoles. When only one multipole is considered for both the gamma rays in the cascade, the mathematical solutions for  $A_2$  and  $A_4$  are unique and the ellipse converges to a point that indicates the single-multipole solution.

The spin assignments to the various levels made from the  $\log ft$  analysis, discussed in Section 3.2.1, have been found also to be corroborating well with the angular-correlation results obtained in the present experiment. For instance, the angular correlation results for the 737-334 keV cascade agrees pretty well with the assigned  $3 \rightarrow 2 \rightarrow 0$  spin sequence. Similar is the case for the 1379-334 keV and 1736-334 keV cascades for which  $3 \rightarrow 2 \rightarrow 0$  and  $2 \rightarrow 2 \rightarrow 0$  spin sequences have, respectively, been proposed in the existing literature. Using the angular correlation results and the  $\log ft$  values,  $J^\pi$  assignment of the 2367.2 keV level has been changed from ( $3^+$ ) to  $2^-$ . This is also supported by the  $\log ft$  analysis and the prediction made in the earlier  $\beta$  decay spectroscopy [6].

The most important observation of the present angular correlation analysis has been the possible assignment of pure  $\Delta I = 0$  (1324, 1736 and 2033 keV) and  $\Delta I = 1$  (832 and 1379 keV) E1

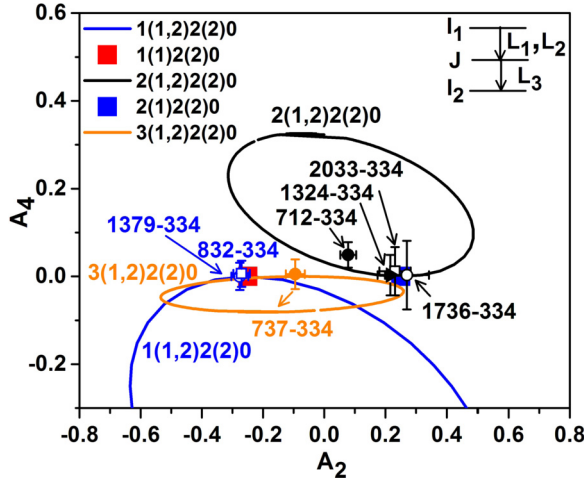


Fig. 9. (Color online.) A comparison between theoretical solutions and the experimental data on  $\gamma - \gamma$  angular correlation associated with the 334.1 keV ( $2_1^+ \rightarrow 0_g^+$ ) E2 transition. Each measured angular correlation value ( $A_2, A_4$ ) has been labeled with the energies of the two coincident gamma rays in keV. The ellipses, labeled according to the convention  $I_1(L_1, L_2)J(L_3)I_2$ , correspond to theoretical solutions of the angular correlations where the first correlated  $\gamma$  is an admixture of two multipoles  $L_1$  and  $L_2$ . The single-multipole solutions are indicated by filled squares. The used convention is illustrated in the upper right corner of the figure.

Table 2

Estimates of possible M2 admixture ( $\delta$ ) and B(E1) strength of the E1 transitions observed in the present work

$E_\gamma$ (keV)	Cascade	Sequence (proposed)	$A_2$	$A_4$	$\delta$	$\frac{B(E1)_\gamma}{B(E1)_{832=2.9(12)}}$ (Expt.) (m W.u.)	B(E1) $_\gamma$ (ap- prox.) (m W.u.)
832	334–832	$1 \rightarrow 2 \rightarrow 0$	$-0.270(27)$	$0.006(30)$	$-0.018(25)$		
1324	334–1324	$2 \rightarrow 2 \rightarrow 0$	$0.216(42)$	$0.003(46)$	$-0.046(35)$	$0.36(9)$	$1.1(5)$
1379	334–1379	$1 \rightarrow 2 \rightarrow 0$	$-0.276(28)$	$0.000(31)$	$-0.024(25)$	$0.06(2)$	$0.16(8)$
1736	334–1736	$2 \rightarrow 2 \rightarrow 0$	$0.270(72)$	$0.003(78)$	$0.028(108)$	$0.06(2)$	$0.16(8)$
2033	334–2033	$2 \rightarrow 2 \rightarrow 0$	$0.231(51)$	$0.012(55)$	$-0.026(19)$	$0.006(1)$	$0.018(8)$

character to five transitions decaying from the five negative parity levels, viz., 1165.5, 1658.2, 1713.3, 2069.7 and 2367.2 keV respectively, to the ground state band. This assignment could be based on the fact that the experimental  $A_2$  and  $A_4$  coefficients for these cascades were close to the single-multipole solutions that are indicated by filled squares in Fig. 9. The negligible M2 admixtures ( $\delta$ ), that might be associated with these transitions are shown Table 2 and it was found to have an upper limit of  $\sim 5\%$ . The results on these five transitions were also compared with the earlier angular correlation measurements [10–12] which have several contradictions among themselves. It is observed that the present results are in line with the work of Kalfas et al. [11], except the high values of M2 admixtures proposed for 1736 and 2033 keV transitions and the ( $3^+$ ) assignment of the 2367.2 keV level. The pure  $\Delta I = 1$ , E1 nature of the 831.5 keV and 1379.2 keV transitions support the spin assignment of the 1165.5 keV and 1713.3 keV levels as  $1^-$ . The  $J^\pi$  assignment of 1165.5 keV level was known from the earlier measurements and that of 1713.3 keV level is assigned in the present work. The E1 nature of the 1324.1, 1735.7 and 2033.1 keV transitions also support the spin assignment of the 1658.2 keV, 2069.7 keV and 2367.2 keV levels, respectively, as  $2^-$ .

With the consideration of E1 nature of the five transitions, viz., 832, 1324, 1379, 1736 and 2033 keV, their B(E1) values can be estimated in comparison to the known B(E1) of the 831.5 keV ( $2.9_{-10}^{+14}$  m W.u. ( $10^{-3}$  W.u.)) [23]  $\gamma$ -ray. The values are shown in Table 2 that have been calculated with the  $B(E1)_{\gamma}/B(E1)_{832}$  ratios obtained from the measured intensity of the respective  $\gamma$ -ray. These estimations might be important for the interpretation on the possible structure of these levels as discussed in the following section.

#### 4. Discussion

A number of low lying positive and negative parity excited levels of  $^{150}\text{Sm}$ , as shown in Table 1 and Fig. 10, are populated from the  $\beta$  decay of  $^{150}\text{Pm}$ . The following two paragraphs are devoted to discuss the systematic observations made and experimental information derived in the present work on few specific positive and negative parity levels in  $^{150}\text{Sm}$ .

The systematics of the  $\beta$  and  $\gamma$  bands observed in the neighboring nuclei has been shown in Fig. 11 including the  $2_3^+$  and  $3_1^+$  states of  $^{150}\text{Sm}$ . Both of the latter two levels of  $^{150}\text{Sm}$  follow this systematics for the  $K = 2$   $\gamma$  phonon structure in the neighboring nuclei and their character is also understood from their similar decay pattern as suggested by Gupta et al. [25].

In the present work, the connection of the 1417.4 keV level to the  $2_2^+$  level of the  $\beta$  band has been established with the placement of the 371.5 keV transition in the level scheme. This finding strongly supports the  $\beta\beta$  character of the 1417.4 keV,  $2_4^+$  level. The 1417.4 keV level also decays to the 1165.5 keV,  $1^-$  level which has a possible octupole structure based on pure E1 nature of the 831.5 keV transition decaying from this level to the 334.1 keV,  $2_1^+$  level.

The pure E1 transitions decaying from some of the negative parity levels have B(E1) strengths ranging from 0.02 m W.u. to 2.9 m W.u., as observed from Table 2. Out of these, high values of the B(E1) strength of 2.9 m W.u. and 1.1 m W.u. for the 831.5 keV ( $\Delta I = 1$ , E1) and 1324.1 keV ( $\Delta I = 0$ , E1) transitions, respectively, indicate a possible octupole vibration involved in the structure of the 1165.5 keV,  $1^-$  and the 1658.4 keV,  $2^-$  levels, when compared to that observed in the neighboring  $^{151}\text{Pm}$  [35].

#### 5. Summary

The decay spectroscopy of  $^{150}\text{Pm}$  has been performed by populating the nucleus with  $^{150}\text{Nd}(p, n\gamma)^{150}\text{Pm}$  reaction at  $E_p = 8.0$  MeV. The observed  $\gamma$ -rays were detected both in singles and coincidence mode with VENUS array having six Compton suppressed Clover HPGe detectors. The decay half lives have been followed for the observed transitions and their  $\gamma - \gamma$  coincidences were studied. The outcome of the present experimental work has been the observation of nineteen new  $\gamma$  transitions and altered placements of eight earlier known transitions resulting in the addition of thirteen new levels of  $^{150}\text{Sm}$  which could be populated from  $\beta$  decay of  $^{150}\text{Pm}$ . The *logft* analyses were performed using the intensities of different  $\gamma$  transitions to determine the  $J^\pi$  assignment for the levels in  $^{150}\text{Sm}$ , populated from  $\beta$  decay. From the *logft* analysis,  $J^\pi$  assignment was made to twenty eight levels for which the assignment was not known or was uncertain. Some of these assignments were also corroborated with the angular correlation measurement which could also confirm the pure E1 nature of five transitions in  $^{150}\text{Sm}$ . The indirectly derived B(E1) values support the octupole character of the 1165.5 and 1658.4 keV levels. The intra- and inter-band E2 transitions from  $2_2^+$  and  $2_3^+$  levels, observed in the present work, suggest that these levels in  $^{150}\text{Sm}$  are the candidates of  $\beta$  and  $\gamma$  vibration bands respectively, in agreement with the evidence in Ref. [22,25]. These levels also follow the systematics in the Ce–Dy isotones

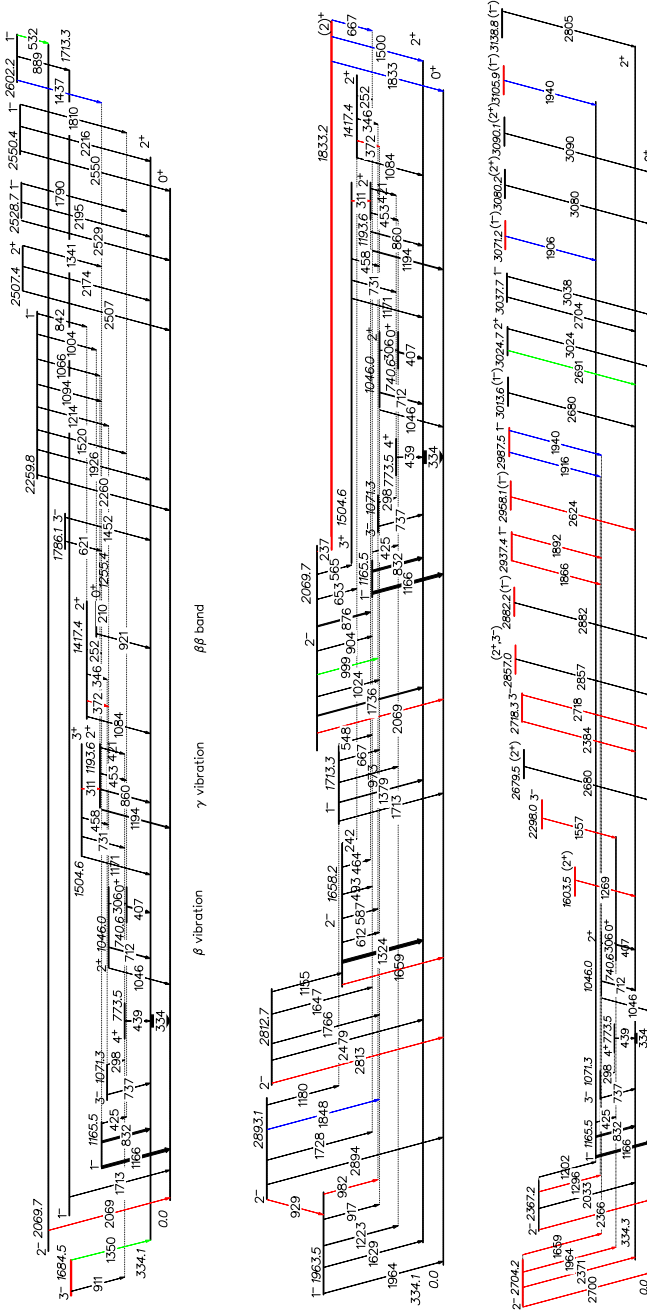


Fig. 10. (Color online.) The partial level scheme for  $^{150}\text{Sm}$ , obtained in the present work following the  $\beta$  decay of  $^{150}\text{Pm}$ , is shown in three parts. Some of the levels are shown in more than one part to completely show the decay and feeding of a particular level. The thirteen new levels placed in the decay scheme and nineteen new transitions found in the present work are shown with red. The transitions for which the placement is altered are shown with blue. The tentative transitions that are confirmed in the present work are shown with green. Some of the levels are shown in bold to increase the visibility.

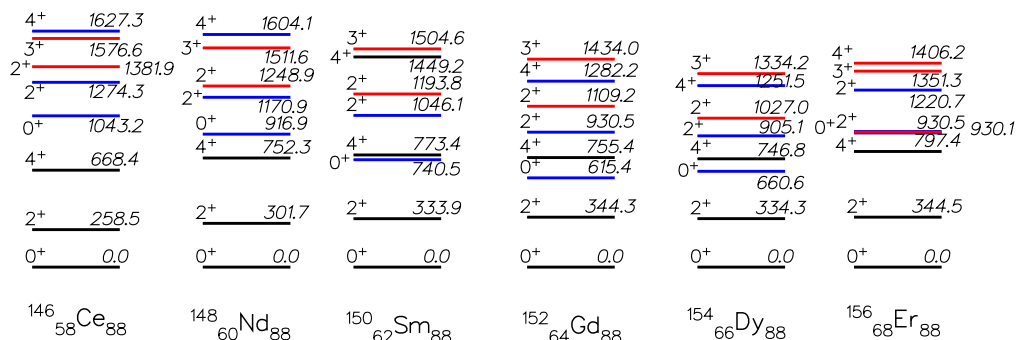


Fig. 11. (Color online.) The systematics of the positive parity low lying levels in  $N = 88$  Ce–Er nuclei. The levels those are assigned to the  $\beta$  band in a nucleus are colored in blue and those to the  $\gamma$  band are colored in red. The level energies are taken from NNDC.

(cf. Fig. 11). The observation of the 371.5 keV E2 transition decaying from the 1417.4 keV,  $2^+_{4+}$  level; which is based on the 1255.4 keV,  $0^+_{3+}$  level; to  $2^+_{\beta}$  level identified in the present work supports the  $\beta\beta$  character of the 1417.4 keV state.

## Acknowledgements

The effort of the staffs and members of the K-130 cyclotron operation group at VECC, Kolkata, is gratefully acknowledged for providing high quality stable proton beam. A. Saha is grateful for his UGC Fellowship (Ref. No:17-06/2012(i)EU-V) for carrying out his experiments at VECC, Kolkata. S. S. Alam would like to acknowledge the support from BRNS fellowship (Sanction No. 2013/38/02-BRNS/1927 for PRF, BRNS, dated 16 October 2013). The efforts of Mr. R. K. Chatterjee, RCD, VECC is acknowledged for target preparation. A. Chowdhury and Shaikh Imran of Physics lab, VECC are acknowledged for their effort to maintain the detectors during experiment.

## References

- [1] Y. Xu, et al., Phys. Rev. Lett. 73 (1994) 2413.
- [2] B. Fogelberg, et al., Phys. Rev. Lett. 68 (1992) 3853.
- [3] A. Lindroth, et al., Phys. Rev. Lett. 82 (1999) 4783.
- [4] E. Nächer, et al., Phys. Rev. Lett. 92 (2004) 232501.
- [5] I. Dillman, et al., Phys. Rev. Lett. 91 (2003) 162503.
- [6] J. Barrette, et al., Can. J. Phys. 48 (1970) 1161.
- [7] B.R. Mottelson, S.G. Nilsson, Phys. Rev. 99 (1955) 615.
- [8] J.B. Gupta, Phys. Rev. C 87 (2013) 064318.
- [9] Singh, Taylor, Z. Phys. A 283 (1977) 21.
- [10] R.K. Smither, Phys. Rev. 150 (1966) 964.
- [11] C.A. Kalfas, A. Xenoulis, T. Paradellis, J. Phys. G 1 (1975) 613.
- [12] E.R. Reddingius, H. Postma, Nucl. Phys. A 137 (1969) 389.
- [13] Masaharu Hoshi, Yasukazu Yoshizawa, J. Phys. Soc. Jpn. 42 (1977) 1106.
- [14] L. Grodzins, B. Herskind, D.R.S. Somayajulu, B. Skalli, Phys. Rev. Lett. 30 (1973) 453.
- [15] Y. Yamazaki, E.B. Shera, M.V. Hoehn, R.M. Steffen, Phys. Rev. C 18 (1978) 1474.
- [16] H.G. Borner, et al., Phys. Rev. C 73 (2006) 034314.
- [17] A. Jungclaus, et al., Phys. Rev. C 48 (1993) 1005.
- [18] W. Andrejtscheff, et al., Phys. Lett. B 437 (1998) 249.

- [19] S.P. Bvumbi, et al., Phys. Rev. C 87 (2013) 044333.
- [20] Krishna Kumar, Nucl. Phys. A 231 (1974) 189.
- [21] O. Scholten, F. Iachello, A. Arima, Ann. Phys. 115 (1978) 325.
- [22] J.B. Gupta, R. Kumar, J. Phys. G 7 (1981) 673.
- [23] S.K. Basu, A.A. Sonzogni, Nucl. Data Sheets 114 (2013) 435.
- [24] <http://www.nndc.bnl.gov/ensdf/xundl/>, last updated on 09-03-2018.
- [25] J.B. Gupta, R. Kumar, K.H. Hamilton, Int. J. Mod. Phys. B 19 (2010) 1491.
- [26] D. Banerjee, et al., Phys. Rev. C 91 (2015) 024617.
- [27] Soumik Bhattacharya, et al., in: Proc. of DAE-BRNS Symposium on Nuclear Physics, vol. 61, 2016, p. 98.
- [28] H. Morinaga, T. Yamazaki, In-Beam Gamma-Ray Spectroscopy, North-Holland Publishing Company, New York, 1976, p. 68.
- [29] <http://www.tifr.res.in/~pell>.
- [30] D.C. Radford, Nucl. Instrum. Methods A 361 (1995) 297.
- [31] P. Humby, et al., Phys. Rev. C 94 (2016) 064314.
- [32] <http://www.nndc.bnl.gov/logft/>.
- [33] D. Bucurescu, et al., Phys. Rev. C 85 (2012) 017304.
- [34] B. Singh, et al., Nucl. Data Sheets 84 (1998) 487.
- [35] W. Urban, Phys. Lett. B 247 (1990) 238.